(Published in Proceedings of TEMPMEKO '99, J. Dubbeldam and M. de Groot, eds., pp. 418-423)

PRIMARY ACOUSTIC THERMOMETER FOR USE UP TO 800 K

D. C. Ripple, D. R. Defibaugh, K. A. Gillis, and M. R. Moldover
National Institute of Standards and Technology, U. S. A.

ABSTRACT

Primary acoustic thermometers determine the thermodynamic temperature of a monatomic gas from measurements of the speed of sound in the gas. Here, we describe the design and construction of an acoustic thermometer designed to operate at temperatures up to 800 K with uncertainties of a few millikelvin. Features of our acoustic thermometer include: construction that minimizes sources of gas contamination; a gas handling system for continuous purging of the resonator during the acoustic measurements; monitoring the purity of the gas exiting the resonator; determination of the thermal expansion and dimensional stability of the resonator cavity by *in situ* measurements of microwave resonance frequencies; use of novel acoustic transducers; and measurement of the temperature of the resonator shell on the International Temperature Scale of 1990 (ITS-90) with up to five long-stem standard platinum resistance thermometers (SPRTs). We are currently in the process of implementing this thermometer at NIST, and results will be presented at a later date.

1. INTRODUCTION AND DESIGN PHILOSOPHY

Thermodynamic temperature measurements using monatomic gases form the basis for the ITS-90 from 273.16 K to 730 K, and provide a reference point for radiometric determinations at higher temperatures [1]. Unfortunately, the best previous measurements [2,3] using Constant Volume Gas Thermometry (CVGT) have discrepancies of 12 mK at 500 K and rising to 30 mK at 730 K, which are much larger than the combined measurement uncertainty.

Thus we were motivated to develop an acoustic thermometer as an alternative technique for determining the thermodynamic temperature above 500 K. In our thermometer, the speed of sound of a monatomic gas is determined from measurements of the frequencies of acoustic resonances in a gas-filled spherical shell of volume V. Kinetic theory relates the speed of sound u to the thermodynamic temperature T. Measurements of the frequencies of microwave resonances within the same shell determine the thermal expansion of the resonator cavity. The equation linking the measured frequencies to T, neglecting small corrections [4, 5], is

$$\frac{T}{T_{\mathrm{w}}} = \left[\frac{u(T)}{u(T_{\mathrm{w}})}\right]^2 = \left[\frac{V(T)}{V(T_{\mathrm{w}})}\right]^{2/3} \left[\frac{f_{\mathrm{a}}(T)}{f_{\mathrm{a}}(T_{\mathrm{w}})}\right]^2 = \left[\frac{f_{\mathrm{m}}(T_{\mathrm{w}})}{f_{\mathrm{m}}(T)}\right]^2 \left[\frac{f_{\mathrm{a}}(T)}{f_{\mathrm{a}}(T_{\mathrm{w}})}\right]^2 \quad , \tag{1}$$

where T_{w} is the triple point of water, 273.16 K, and f_{a} and f_{m} are acoustic and microwave resonance frequencies.

Distinct advantages of acoustic thermometry over earlier CVGT work include higher precision, the ability to conduct experiments with continuously flowing gas, and the ability to use microwave resonances to characterize the volume of the resonator cavity *in situ*. Recent acoustic thermometry results [4,5] at NIST have determined thermodynamic temperature to a standard uncertainty of 0.6 mK in the temperature range 217 K to 303 K. The present NIST effort seeks to greatly expand the temperature range of precision acoustic thermometry and to benefit from the lessons learned while conducting the lower temperature measurements. The NIST acoustic thermometer, shown in Fig.1, has the following features:

A. Operation up to 800 K. Discrepancies between the NBS/NIST CVGT data become significant at temperatures above 500 K. Measurements at the zinc freezing point (692.677 K) are desirable, because the determined value of $(T - T_{90})$ at the fixed-point temperatures does not depend on the nonuniqueness of the SPRTs, which is a measure of the interpolation error between fixed points on the ITS-90.

B. Continuous purging of the resonator cavity. Contamination of the gas in the resonator is proportional to its residence time, or inversely proportional to flow rate. Continuous purging reduces gas residence time approximately two orders of magnitude relative to the residence time in CVGT experiments.

C. Direct measurement of impurities in the gas exiting the resonator.

D. Simultaneous microwave and acoustic measurements. At elevated temperatures, creep of the spherical shell is a significant possibility. Microwave measurements that are concurrent with the acoustic measurements test for creep at each datum point.

E. Stable and inert materials. We use no elastomers, which have been a significant source of outgassing in previous acoustic thermometers.

F. Removable thermometers calibrated on the ITS-90. Removable thermometers allow periodic checks at T_w and easier determination of thermal gradients.

G. A resonator cavity of approximately 3 L. Previous measurements with cavity volumes of 1 L or less have halfwidths of the acoustic resonances that are larger than predicted by theory.

Figure 1. Simplified cross section of the 3 L resonator, the pressure vessel, and associated plumbing and electrical connections. The furnace surrounding the pressure vessel is not shown.

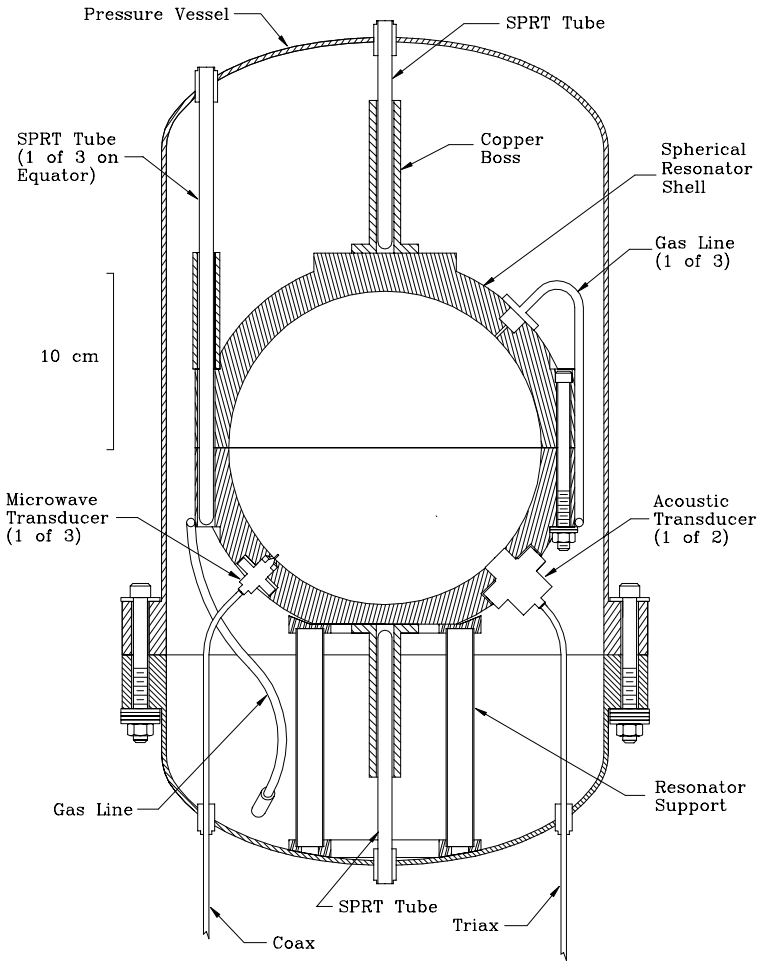

2. MATERIALS FOR HIGH TEMPERATURE OPERATION

All components of the NIST acoustic thermometer are constructed of materials that are dimensionally stable at 800 K and that have inherently low outgassing rates. The materials exposed to high temperatures include: stainless steel (SS), copper, alumina, boron nitride, platinum, and gold. The choice of a material for the spherical shell itself requires consideration of several additional properties: the resonator cavity must maintain a nearly spherical shape at all temperatures, and any oxide layer on the cavity wall must be stable.

The dimensional stability of candidate materials for the spherical shell (copper, 316 L stainless steel, nickel 201, and monel) was studied by measuring the change in flatness of rectangular blocks that were held at 800 K in flowing argon for one week. All samples remained flat to within the resolution of 15 μm over 10 cm. In another experiment, the mass change of copper and stainless steel foils held at 780 K for one week in flowing argon was less than the equivalent of 1 nm of oxide growth, which would result in a negligible change in a.

At high temperatures, creep and anisotropic thermal expansion of the spherical shell can lead to an angle-dependent deformation Δa in the radius a of the resonator cavity. Scaling the acoustic frequencies by the average of the microwave resonance frequencies corrects for any temperature variation in the average value of a and for

deformations of the sphere to first order in $\Delta a/a$ [6]. However, there are effects in the second order of $\Delta a/a$ that are not corrected. Therefore, measuring the speed of sound with a relative uncertainty of 10^{-6} requires stability of the order 10^{-3} for $\Delta a/a$, or 90 μm for a = 9 cm, the cavity radius of our acoustic resonator.

The experiments described above demonstrated that the candidate metals had adequate dimensional and chemical stability, so secondary considerations determined the choice of material for the spherical shell. Because ferromagnetism has undesirable effects on the microwave resonances, nickel was excluded. Monel, and to some extent copper, are difficult to machine. Stainless steel has excellent mechanical properties, but poor thermal conductivity. Because calculations demonstrated that thermal conductivity of the shell was not critical, we chose to use the same shell, fabricated from 316L SS, that has been used for previous thermometry work, after modifying it to accommodate new transducers, gas ports, and long-stem SPRTs.

3. ACOUSTIC MEASUREMENTS WITH CONTINUOUS GAS FLOW

There are three requirements when making acoustic measurements with continuous gas flow: (a) the pressure must be sufficiently stable such that adiabatic temperature variations in the gas are small, (b) the difference between the temperatures of the gas and of the shell wall must be small, and (c) the gas line must not significantly perturb the acoustic resonances.

A fractional change in gas pressure, $\Delta p/p$, will induce an adiabatic change in the gas temperature inside the resonator cavity of $\Delta T/T = ((\gamma - 1)/\gamma)(\Delta p/p)$, where $\gamma = 5/3$ is the specific heat ratio of the gas. Requiring temperature stability of 0.5 mK at 800 K leads to the requirement of a fractional pressure stability of 1.6×10^{-6} for time scales shorter than the thermal diffusion time of the gas in the resonator cavity, approximately 100 s. We have achieved stabilities substantially better than this with a two-stage pressure regulation system upstream of the spherical shell. The gas pressure is first regulated with a standard diaphragm-type regulator. To enable a very fine adjustment of the flow rate, gas flowing from the regulator is then split, with approximately 90% of the gas flowing through a capillary tube and the remaining 10% of the gas flowing through an electromagnetic flow-control valve. A PID loop adjusts flow through the control valve to maintain a constant pressure of the gas in the resonator. The pressure is measured with a quartz Bourdon-tube gauge and a capacitance-type differential pressure transducer separating the Bourdon gauge from the gas inside the shell. Downstream of the resonator cavity, the gas passes through a leak valve to a vacuum pump. Typical flow rates for our thermometer are 3×10^{-5} mol/s to 3×10^{-4} mol/s.

Thermal equilibrium of the gas with the walls of the spherical shell is attained by straightforward techniques of thermally anchoring the gas lines to two of the shells of the furnace, and to the equatorial region of the spherical shell. All gas lines have bends at the inner and outer furnace shells to reduce heat transfer by thermal radiation.

The aperture of the gas line into the spherical shell must be large enough so that the gas flow does not become highly turbulent, because acoustic noise generated by turbulence increases as the eighth power of the Reynolds number. A large aperture, however, can acoustically couple the resonance volume to the gas line. As suggested in Ref. [7], each gas line opens into a volume of approximately 1 cm^3 at the wall of the spherical shell, and a small duct of length $a/10$ connects this volume with the resonator cavity, as shown in the upper right of Fig. 1. This geometry acts as a low-pass acoustic filter, preventing significant shifts of the acoustic resonance frequencies. A bore diameter of 1.5 mm does not significantly perturb the acoustic resonance frequencies and is large enough to create minimal turbulence. The gas entrance and exit apertures are not diametrically opposite one another. If they were, inadequate mixing might occur, because at high Reynolds numbers, the gas flows out of the small duct into the shell as a collimated jet.

4. MINIMIZATION AND MEASUREMENT OF GAS IMPURITIES

Impurities in the gas in the resonator cavity alter $u(T)$, with consequent errors in T. Therefore, we have designed our apparatus to minimize the quantity of impurities, and we confirm the purity of the gas leaving the resonator by direct measurement of impurities and indirect tests of the effects of impurities.

There are three potential sources of impurities: impurities in the source gas, outgassing from thermometer materials, and permeation of laboratory air through the pressure vessel. The purity level of commercially-supplied research grade argon (99.9999%) is sufficient for our needs. The primary concerns are contamination by

outgassing of materials in contact with the gas and permeation of laboratory air through the pressure vessel. The spherical shell, the accompanying transducers and feedthroughs, and virtually all of the gas handling system are constructed from metals and hard-fired ceramics. There are no elastomers in the gas handling system. At 800 K, hydrogen readily permeates stainless steel [8]. As a result, the dominant impurity at high temperatures is expected to be hydrogen.

The purity of the gas exiting the cavity will be verified by routing the exiting gas to a customized gas chromatography system capable of detecting hydrogen, nitrogen, carbon monoxide, carbon dioxide, and hydrocarbons at a level of $0.3H10^{-6}$ mole fraction. If an impurity is present in the resonator cavity, the resonance frequencies will be shifted by an amount proportional to the impurity concentration. In a continuously purged system contaminated by gas permeation and outgassing, the impurity concentration is inversely proportional to flow rate. The most important test of the presence of impurities, then, is to monitor the resonance frequency of an acoustic mode while varying the flow rate of gas through the resonator cavity.

5. ACOUSTIC AND MICROWAVE TRANSDUCERS

Excitation and detection of the acoustic modes require acoustic transducers that can operate reliably at 800 K, have noise levels no larger than the equivalent of 10^{-5} Pa/Hz$^{1/2}$, have a smooth frequency response from 2.5 kHz to approximately 17 kHz, and that do not appreciably perturb the frequencies of the acoustic resonances. For operation at room temperature, the ideal transducers are capacitance microphones, which have a thin membrane spaced approximately 40 μm from a back electrode. In the detection mode, sound waves deflect the membrane, altering the capacitance between the two electrodes.

For operation at 800 K, no commercial transducers exist that meet our requirements, so we fabricated our own capacitance transducers, as shown in Fig. 2. The membrane is a square of monocrystalline silicon, approximately 25 μm thick. This membrane fits in the well of a photoetched stainless steel disk that also serves as a spacer to maintain a 40 μm gap between a back SS electrode and the silicon. The back electrode is set into a ceramic insulator fabricated from machinable alumina. These transducers have low outgassing, good dimensional stability at high temperatures, and a smooth frequency response from 0.5 kHz to 18 kHz.

Figure 2. Simplified cross sections of the acoustic and microwave transducers.

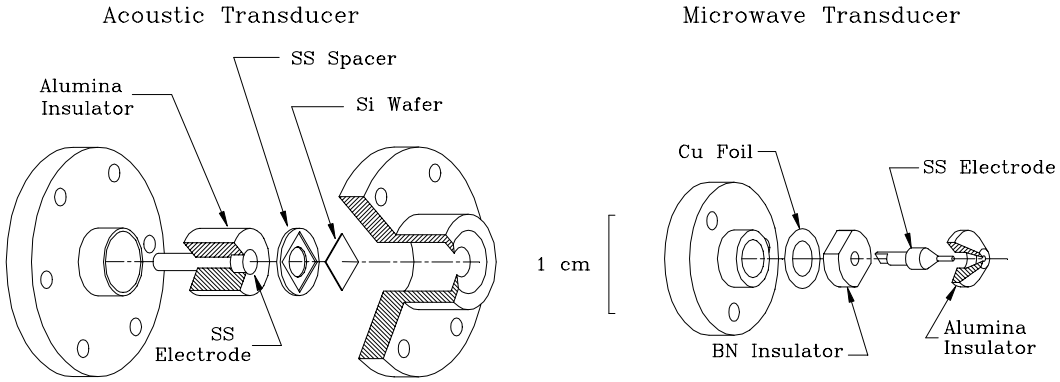

The total capacitance of the transducer is of the order of only 3 pF. To achieve adequate sensitivity, it is necessary to use triaxial cable from the transducer, out of the furnace, through a hermetic feedthrough, and to the preamplifier. The triaxial cable from the transducer to the seal is constructed from two concentric stainless steel tubes and an inner platinum conductor, all insulated from each other by alumina tubes.

The variation of the volume of the resonator cavity with temperature is determined from measurements of the center frequencies of microwave resonances as a function of temperature. As in Ref. [4], we choose to measure only transverse magnetic (TM) triplets (l=1), which couple to a simple pin transducer. The microwave resonances are measured with a network analyzer, connected to the spherical shell with coaxial cable terminated at the shell wall with a 3 mm long pin. As with the acoustic transducers, homemade coaxial cable constructed of Pt wire, an alumina tube, and an outer SS tube integral with the pressure vessel carries the microwaves from the transducers to a hermetic feedthrough at room temperature. Because of the high quality factor of the microwave resonances (approximately 10^4), the impedance mismatches between the transducer, the coaxial line, and the

hermetic feedthrough do not significantly affect the resonant frequencies. With this configuration, we are able to measure the resonant frequencies of the three lowest TM triplets at frequencies of 1.47 GHz, 3.28 GHz, and 5.00 GHz with a relative uncertainty of approximately 10^{-7}. The resulting relative uncertainty in T is several parts in 10^7, as derived from Eq. 1.

The resonant frequency of a given microwave mode is not equally sensitive to all deformations of the resonator cavity. However, it has been shown, theoretically and experimentally [6], that the effective volume for radial acoustic modes is equivalent to the average of the effective volume for all components of a microwave multiplet. The particular cavity of the NIST acoustic thermometer is slightly oblong along the z axis. Consequently, one mode of each TM triplet is split from the other two modes. The doublet cannot be resolved, but it is necessary to insure that the measurements equally weight the two degenerate modes in the determination of the average resonant frequency. This is accomplished by measuring the frequencies of the microwave resonances twice, using two transducers in turn as sources and a third transducer as a detector for both measurements. The two sources are separated by 90° in the x-y plane, with one source in the x-z plane and one in the y-z plane. Assuming that the doublet splitting is much less than the resonance halfwidth, a mixture of both doublet modes is excited by a point source, with the resulting mixed mode having symmetry about the x or y axis. Both sources also excite the mode with z-axis symmetry. From measurements with both sources, the deformations of the resonator cavity can be probed with modes in all three spatial directions: x, y, and z.

6. THERMOMETRY ON THE ITS-90 AND THE THERMAL ENCLOSURE

Accurate measurements of T require that the spherical resonator, including the gas in the cavity, be maintained at a uniform and stable temperature. Accurate measurements of T_{90} additionally require that the SPRTs be in thermal equilibrium with the wall of the spherical shell. To meet these requirements, the pressure vessel is encased in three concentric aluminum shells that are actively temperature controlled, and the thermal coupling between the aluminum shells, the SPRTs, and the spherical resonator have been carefully modeled.

The wall temperature of the spherical shell can be measured by up to five long-stem, 25.5 Ω SPRTs. As shown in Fig. 1, the pressure vessel has five tubes welded into its walls that slide into copper bosses located at the top, bottom, and equator of the spherical shell. The SPRTs are placed inside these tubes, and the SPRTs may readily be removed while the furnace is at high temperature for the purposes of checking the T_w resistance ratio or interchanging SPRT positions. Thermal gradients along the SPRT tubes can be mapped by adjusting the SPRT position inside the tubes. As an additional check on the gradients in the shell wall, a thermopile made from Pt and Cu-Ni thermoelements has been installed, with junctions at the equator of the shell and at a position midway between the equator and the top of the shell. By annealing the Pt thermoelements that pass from room temperature to the spherical shell in the same manner as used for Au/Pt thermocouples, the Pt leads introduce no more than 0.05 μV stray thermal emf, equivalent to a 0.5 mK error.

The size of the pressure vessel is determined by the requirement that the SPRTs must have sufficient immersion depth into a region nearly the same temperature as the shell to avoid significant sheath losses. Plots of SPRT response on immersion into zinc freezing-point cells show that sheath losses are minimal if a 14.5 cm length of the SPRT from the tip is within approximately 10 mK of the sensing element temperature. The resulting pressure vessel is 25.4 cm in diameter and 47 cm long, with elliptical top and bottom ends, and a flange near the bottom end that is sealed with a gold wire o-ring. The aluminum shell surrounding the pressure vessel has a minimum thickness of 1 cm, and additional aluminum bosses are used around the SPRT ports to increase the near-isothermal length of each SPRT to 14.5 cm.

For aluminum shells large enough to encase the pressure vessel, a simple thermal model based on "lump elements" of the thermal resistance of the furnace shell and of the insulation is not appropriate. The thermal model must account for the flow of heat both along the shells and across the insulation between shells. A simple analytical model suffices for design purposes and demonstrates that adding control points, each with an independent temperature sensor and heater, is an effective way of improving the thermal uniformity of a furnace. Consider a metal plate of conductivity λ_m and thickness d_m is spaced a distance d_i from a flat substrate by a layer of insulation of thermal conductivity λ_i. If the temperature profile on the substrate varies along its length as $A_s \sin(kx)$, then in the limit of $kd_i \ll 1$ the ratio of the imposed temperature variation on the metal plate to the variation on the substrate is

$$R_{ms} = A_m / A_s = \frac{1}{1+(k\alpha)^2}, \ \alpha = \sqrt{\lambda_m d_m d_i / \lambda_i} \quad (3)$$

High values of α or of k result in strong attenuation of temperature fluctuations. The strong dependence of R_{ms} on k indicates that with several metal shells, the thermal gradients on the innermost shell will be dominated by the spatial fluctuations corresponding to the longest lengths, or the smallest k values. The variable x can be imagined to follow a path around the circumference of the shell at its widest dimension. With a shell circumference of C, and a single temperature control point, the periodicity of the temperature gradients requires $k=2\pi n/C$, $n=1, 2, ...$ Increasing the number of control points to N_{cp}, and spacing them equally, gives $k_{min} = 2\pi N_{cp}/C$. Using this method, we have designed the shells to give a ratio of thermal gradients on the outer aluminum shell to those on the inner shell of 900. The inner and outer shells have three control points each.

The accuracy and stability of the temperature at the control points of the innermost aluminum shell is critical for the success of the experiment. We use Au/Pt thermocouples as sensors on the shell. The uncertainty of such sensors is approximately 10 mK, thermocouples made from a single lot of wire are highly interchangeable, and stability tests have indicated no measurable drift for 1000 hours of use at temperatures up to 1235 K. Nanovoltmeters are used to read each Au/Pt thermocouple, and the analog output of each nanovoltmeter is configured to be equal to the amplified difference of the thermocouple emf and a setpoint voltage. The analog output is fed into a standard PID controller that in turn controls the DC power supplies of the shell heaters.

7. CONCLUSIONS

The acoustic thermometer described above has been constructed at NIST, and testing of the thermometer is in progress. The standard uncertainties at 800 K are expected to be approximately 3 mK to 5 mK.

REFERENCES

[1] Rusby, R. L., Hudson, R. P., Durieux, M., Schooley, J. F., Steur, P. P. M., and Swenson, C. A., *Thermodynamic Basis of the ITS-90*, Metrologia, 1992, **28**, pp. 9..18

[2] Guildner, L. A. and Edsinger, R. E., *Deviation of the International Practical Temperatures from Thermodynamic Temperatures in the Temperature Range from 273.16 K to 730 K*, J. Res. Natl. Bur. Stand. (U.S.) Sec. A, 1976, **80**, pp. 703..737

[3] Edsinger, R. E. and Schooley, J. F., *Differences between Thermodynamic Temperature and t (IPTS-68) in the Range 230 °C to 660 °C*, Metrologia, 1989, **26**, pp. 95-106

[4] Moldover, M. R., Boyes, S. J., Meyer, C. W., and Goodwin, A. R.. H., *Thermodynamic Temperatures of the Triple Points of Mercury and Gallium and in the Interval 217 K to 303 K*, J. Res. Natl. Inst. Stand. Technol., 1999, **104**, pp. 11..46

[5] Moldover, M. R., Boyes, S. J., Meyer, C. W., and Goodwin, A. R.. H., *Primary Acoustic Thermometry from 217 K to 303 K*, paper presented at this symposium

[6] Ewing, M. B., Mehl, J. B., Moldover, M. R. and Trusler, J. P. M., *Microwave Measurements of the thermal expansion of a spherical cavity*, Metrologia, 1988, **25**, pp. 211..219

[7] Goodwin, A. R. H., *Thermophysical Properties from the Speed of Sound*, Ph. D. Thesis, University College London, 1988, pp. 113..117

[8] O'Hanlon, John F., *A User's Guide to Vacuum Technology,* Wiley & Sons, New York, 1980, p. 150

Address correspondence to: Dean Ripple, NIST, 100 Bureau Dr., Stop 8363, Gaithersburg, MD 20899-8363